In the absence of a probe input to the DOPA, the device produces a squeezed vacuum with noise properties that are investigated by interfering it with a coherent local oscillator (LO) at the homodyne detector. As the relative phase between the LO and squeezed vacuum fields was scanned, we measured directly up to 0.5 dB of noise reduction below the shot noise level (Fig. 2). The factor that had the greatest effect on the experimental observation of vacuum squeezing was the temporal mismatch between the LO and squeezed pulses. Once this factor, along with propagation and detector losses, has been considered, the measured noise reduction of 0.5 dB implies 1.8 dB of actual squeezing generated by the DOPA.

We are presently investigating the efficiency of second-harmonic generation using a superposition of squeezed vacuum and a coherent beam from the laser.[4] We expect the intensity of the doubled light (I_{SHG}) to be modified in such a way that depends upon the relative phase (θ) between the coherent and squeezed fields

$$I_{SHG} \sim I_C^2 + 2I_C I_{SV}\{2 + \cos(2\theta)\}$$

where I_C and I_{SV} are the intensities of the coherent and squeezed components of the beam, respectively. A schematic of the experimental setup is shown in Fig. 3. We will report on our experimental attempt to observe this phenomenon.

Present address: Fakultät für Physik, Universität Konstanz, 78343 Konstanz, Germany

1. G.P.A. Malcolm, P.F. Curley, A.I. Ferguson, Opt. Lett. **15,** 1303 (1990).
2. H.P. Yeun, V.W.S. Chan, Opt. Lett. **8,** 177 (1983); G.L. Abbas, V.W.S. Chan, T.K. Yee, Opt. Lett. **8,** 419 (1983); B.L. Schumaker, Opt. Lett. **9,** 189 (1984).
3. P. Kumar, O. Aytür, J. Huang, Phys. Rev. Lett. **64,** 1015 (1990).
4. J. Gea-Banacloche, Phys. Rev. Lett. **62,** 1603 (1989).

QWF38

Optical pumping-induced population grating transfer in cold cesium atoms

G.C. Cardoso, V.R. Carvalho, S.S. Vianna, J.W.R. Tabosa, *Departamento de Física, Universidade Federal de Pernambuco, 50670-901 Recife, PE, Brasil*

Four-wave mixing (FWM) is an important holographic technique to study the process of writing and reading of a dynamic grating in a nonlinear medium.[1] Recently, several groups have demonstrated a different type of laser-induced dynamic gratings, the so-called optical lattices,[2] which can trap atoms in a three-dimensional spatial structure. The use of cold atoms to perform FWM is a well-related phenomenon, since in this regime the induced population or polarization gratings by the FWM beams are basically not affected by the atomic motion and this can also lead to a long-lived spatial modulation of some local atomic variables.

We report on the observation of nondegenerate four-wave mixing (NDFWM) in cold atoms via optical pumping-induced population grating transfer between the hyperfine levels of cesium D_2 line. Our experiment was performed with cold cesium atoms using the experimental scheme depicted in Fig. 1a. The forward (F) pump and the probe (P) beams have the same frequency ω_1, while the backward (B) has a frequency ω_2. The generated phase conjugate (PC) beam, which is nearly counterpropagating with the probe beam, is directly detected by a photodiode. In Fig. 2a and b we show, respectively, the probe beam absorption and PC spectra when the frequency ω_2 is resonant with the $6S_{1/2}$, F = 3 − $P_{3/2}$, F′ = 2 transition and the frequency ω_1 is tuned around the $6S_{1/2}$, F = 4 − $6P_{3/2}$, F′ = 3, 4, 5 transitions, according to the level scheme shown in Fig. 1b. As indicated, we only can observe the NDFWM signal when the frequency ω_1 is resonant with a noncycling transition,[3] thus evidential of the grating transfer mechanism. The grating induced by F and P beams is transfered via spontaneous emission to the lower hyperfine ground state from where the B beam is diffracted.

We also have demonstrated the use of the NDFWM process for image processing with nearly degenerate frequency conversion and for wave-front rectification. In Fig. 3a we show a CCD image of the probe beam in which was impressed the characteristics fringes patterns. In Fig. 3b we show the image of the diffracted beam generated by the NDFWM process. These images clearly reveal that the image impressed onto the probe beam oscillating at a frequency ω_1 was transfered to the nearly degenerate diffracted beam at frequency ω_2. Furthermore, we have also demonstrated that our system can perform wave-front reconstruction by placing a phase aberrator in the way of the probe beam, thus generating the image shown in Fig. 3c. Figure 3d shows the rectified image. These remarkable effects can be achieved for large angular aperture between the "object" probe (P) beam and the forward (F) pump beam (up to $\theta \sim 65°$). From another point of view, the grating transfer mechanism itself can be used to perform a nondestructive prospect

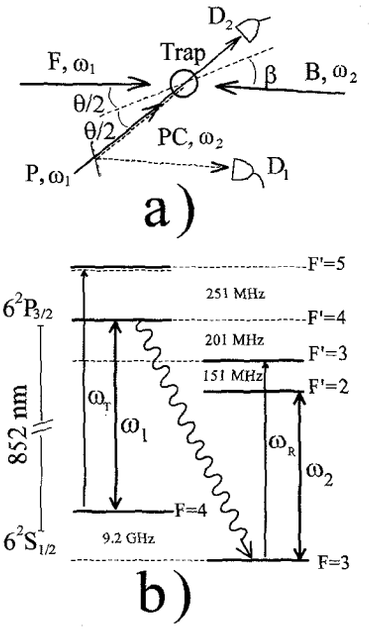

QWF38 Fig. 1. (a) Experimental beam arrangement for observing the NDFWM signal. The forward (F) and the probe (P) beam have the same frequency ω_1, while the backward (B) beam has frequency ω_2. (b) Hyperfine energy levels of cesium D_2 line. The arrows indicate the lasers interacting with the corresponding transitions, i.e., the trapping, the repumping and the FWM beams.

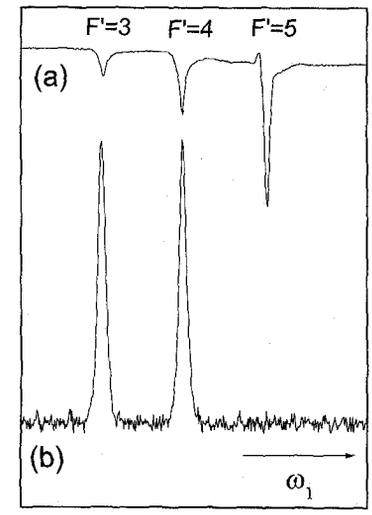

QWF38 Fig. 2. (a) Probe beam absorption spectrum around the transition $6S_{1/2}$, F=4 − $6P_{3/2}$, F′=3, 4, 5. (b) NDFWM spectrum for linear parallel polarizations of the F, P, and B beams. For this spectrum, the frequency ω_2 is resonant with the transition F=3 − F′=2, while the ω_1 is scanned around the transition F=4 − F′=3, 4, 5.

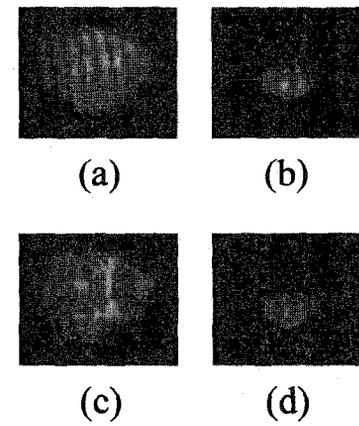

QWF38 Fig. 3. (a) CCD recording of the probe beam spatial profile obtained by reflecting it from a uncoated beam splitter. This image is obtained by retroreflecting the probe beam with plane mirror placed near (~ 15 cm) to the trap, while the CCD camera is located about 2 m away. (b) Diffracted beam profile, at frequency ω_2, evidential of the spatial structure impressed in the probe beam at frequency ω_1. (c) Probe beam image on the same condition as in (a), but with a phase aberrator in the probe path. (d) Diffracted beam image in the presence of the aberrator. The wave-front distortions are rectified after the generated signal travels back through the aberrator.

of the trap dynamics. In particular, the angular dependence of the NDFWM signal, which can give information on the velocity distribution in the trap environment, will be discussed.

1. H.J. Eichler, P. Lünter, D.W. Pohl, *Laser Induced Dynamics Gratings* (Springer-Verlag, 1985).
2. G. Grynberg, B. Lounis, P. Verkerk, J.-Y. Courtois, C. Salomon, Phys. Rev. Lett. **70,** 2249 (1993); A. Hemmerich, C. Zimmermann, T. Hänsch, *ibid.* **22,** 89 (1993); G. Birkl, M. Gatzke, I.H. Deutsch, S.L. Rolston, W.D. Phillips, *ibid.* **75,** 2823 (1995); M. Weidemüller, A. Hemmerich, A. Görlitz, T. Esslinger, T.W. Hänsch, *ibid.* **75,** 4583 (1995).
3. J.W.R. Tabosa, S.S. Vianna, F.A.M. de Oliveira, Phys. Rev. **A55,** 2968 (1997).

QWG

2:30 pm–4:00 pm
Room 200–212

Coherence Effects in Gain and Loss I

J.P. Marangos, *Imperial College of Science and Technology, United Kingdom, Presider*

QWG1 (Invited) **2:30 pm**

Electromagnetically induced transparency with spectator momenta

Hui Xia, S.J. Sharpe, A.J. Merriam, G.Y. Yin, S.E. Harris, *Edward L. Ginzton Laboratory, Stanford University, Stanford, California 94305*

The prototype situation for both coherent population trapping and electromagnetically induced transparency (EIT) occurs in an ideal three-state atom (Fig. 1a). But, most often, atoms have additional angular momenta that enlarge the manifold of coupled states. An example of this is ^{207}Pb, where a nuclear spin of I = 1/2 splits the fine structure levels of spin-free ^{208}Pb into their hyperfine components (Fig. 1b). Even though a particular three-state subsystem may be made transparent, other subsystems will produce a prohibitively large change in the complex refractive index, and the medium will be opaque. We show that, to obtain transparency and near unity refractive index, instead of tuning the lasers to a Raman-like subset of the split transitions, one should tune the lasers to the centers of gravity of the splittings that are caused by the spectator momentum. We also report the first demonstration of EIT with pulsed lasers in an optically thick sample of atoms which exhibit hyperfine structure using this approach.

We obtain the real and imaginary parts of the dipole moment for the multistate system by weak probe perturbation theory and numerical simulations. With the lasers tuned to the centers of gravity of the transitions, the dipole moment at the probe frequency is zero to first order. The first-order zero in the dipole moment occurs on an atom-by-atom basis when linear polarized laser fields are applied; if circularly polarized laser fields are employed, the first-order zero dipole moment again is observed, but due to a macroscopic cancellation of single-atom dipole moments. We have used orthogonal circular polarizations in the experiment described below.

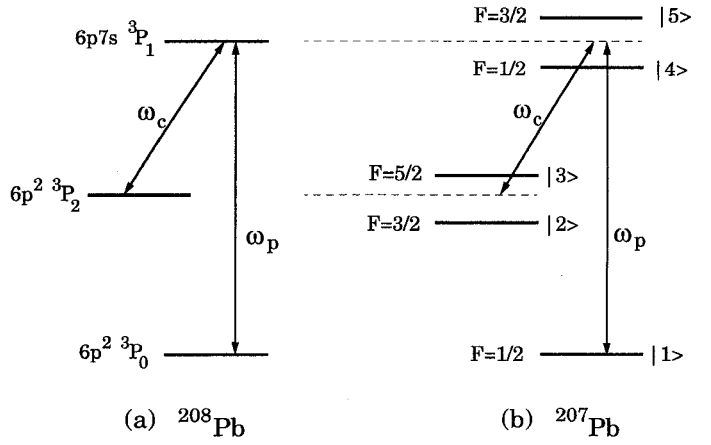

QWG1 Fig. 1. Energy schematic for (a) ^{208}Pb and (b) ^{207}Pb. The nuclear spin of ^{208}Pb is zero and there is no hyperfine splitting. The center of gravity of the hyperfine split levels of ^{207}Pb are shown relative to the level frequencies of ^{208}Pb.

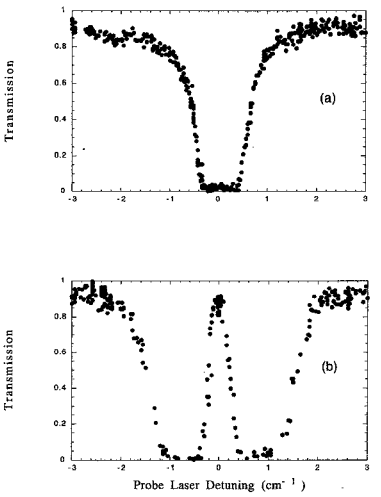

QWG1 Fig. 2. Transmission versus probe laser frequency in ^{207}Pb vapor. (a) Probe alone, no coupling laser present. (b) A coupling laser with Rabi frequency 1.7 cm^{-1} is applied and tuned to the center of gravity of the 6p^2 $^3P_2$ → 6p7s $^3P_1$ transition.

We work with 92% ^{207}Pb vapor filled in a 10-cm long fused-silica side-arm cell at a typical density of 4×10^{14} atoms/cm^3. We apply a 283 nm "probe" laser to the 6p^2 $^3P_0$ → 6p7s $^3P_1$ transition and a 406 nm "coupling" laser to the 6p^2 $^3P_2$ → 6p7s $^3P_1$ transition. We determine the respective center of gravities of the two transitions in ^{207}Pb via a reference cell filled with 99% isotopically pure ^{208}Pb.

Figure 2 shows the transmission of the probe laser versus probe frequency. The coupling laser frequency was fixed at the center of gravity of the 6p^2 $^3P_2$ → 6p7s $^3P_1$ transition, and the probe laser was tuned. As predicted from numerical simulation, 90% transmission was obtained at line center.

We study the refractive index caused by ^{207}Pb by looking at the diffraction pattern of the spatially structured probe laser after it propagates through the ^{207}Pb cell. Applying a coupling laser with Rabi frequency of 1.7 cm^{-1}, and tuning both lasers to the respective center of gravity of each transition results in a diffraction pattern (Fig. 3b) very close to the case of free space propagation (Fig. 3a). If we instead tune the lasers to the Raman resonance

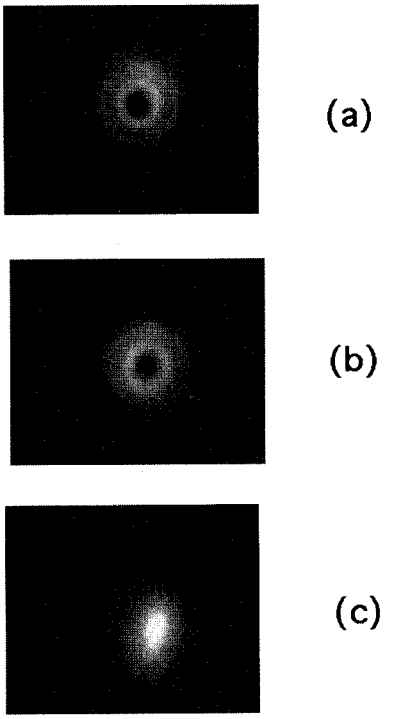

QWG1 Fig. 3. Images of the diffraction patterns of the probe beam after passage through the ^{207}Pb cell. (a) Probe alone in a cold cell. (b) ^{207}Pb density = 4×10^{14} atoms/cm^3 with a coupling laser of Rabi frequency 1.7 cm^{-1} applied and both lasers tuned to the respective center of gravity of the transitions. (c) The same condition as in (b) except that the two lasers are tuned to Raman resonance of a three-state subsystem (coupling laser resonant with the 6p^2 $^3P_2$, F = 5/2 → 6p7s $^3P_1$, F = 3/2 transitions, probe laser resonant with 6p^2 $^3P_0$, F = 1/2 → 6p7s $^3P_1$, F = 3/2). [In (a), (b) and (c), the Rabi frequency of the probe laser is 0.1 cm^{-1}.]